

# Interactions between Organized, Surface-Confined Monolayers and Vapor-Phase Probe Molecules. 9. Structure/Reactivity Relationship between Three Surface-Confined Isomers of Mercaptobenzoic Acid and Vapor-Phase Decylamine

Mona Wells, Daniel L. Dermody, Huey C. Yang, Taisun Kim, and Richard M. Crooks\*,†

Department of Chemistry, Texas A&M University, College Station, Texas 77843-3255

Antonio J. Ricco\*,‡

Microsensor Research and Development Department, Sandia National Laboratories, Albuquerque, New Mexico 87185-1425

Received September 25, 1995<sup>⊗</sup>

We used Fourier transform infrared external reflectance spectroscopy (FTIR-ERS), nanogravimetry based on thickness-shear-mode resonators (TSMRs), and X-ray photoelectron spectroscopy (XPS) to study self-assembled monolayers (SAMs) of three mercaptobenzoic acid (MBA) isomers on Au and their interactions with vapor-phase decylamine. FTIR-ERS spectra of the 4-, 3-, and 2-MBA SAMs indicate that the proximity of the carboxylic acid group to the Au substrate surface affects the electronic environment of the benzene ring and the acidity of the carboxyl-group proton. TSMR results show that reaction of 4-, 3-, and 2-MBA monolayers with vapor-phase decylamine probe molecules results in decylamine fractional surface coverages of 0.97, 0.83, and 0.45 of the theoretical monolayer maximum, respectively. The gravimetric results are corroborated by *in-situ* FTIR-ERS difference spectra of the MBA monolayers obtained during reaction with decylamine, which show the simultaneous disappearance of carbonyl and hydroxyl bands and appearance of carboxylate and aliphatic hydrocarbon bands. XPS results show that increasing the proximity of the carboxyl group to the surface results in a relative increase in the proportion of carboxyl-group oxygen that is in the 531.0 eV electron binding energy state compared to the 532.5 eV state, indicating a change of chemical environment for oxygen. The overall results are consistent with a model involving proton transfer from the SAM to the vapor-phase bases wherein acid strength depends on the accessibility of the donor group, and they demonstrate a clear structure/reactivity correlation for surface-confined isomers, which illustrates the dramatic constraints imposed by surface-induced ordering compared to anisotropic bulk-phase reactivity.

## Introduction

Here we report the first example of a difference in the chemical reactivity of self-assembled monolayers (SAMs) prepared from different isomers of the same molecule. We illustrate a structure/function relationship between the different isomers by monitoring the reactivity of the vapor-phase probe decylamine with SAMs prepared from each of three mercaptobenzoic acid (MBA) isomers. Scheme 1 summarizes our principal findings: the 4- and 3-MBA isomers have surface-accessible hydroxyl groups, and they are both receptive to proton-transfer reactions with vapor-phase decylamine. However, the 2-MBA acid group is located close to the substrate surface and interacts to a lesser extent with decylamine than with the other two isomers. These results illustrate the influence of monolayer structure on surface reactivity, and they contrast strongly with the anisotropic reactivity demonstrated by bulk-phase molecules.

Previous work related to interactions between organomercaptan-based SAMs confined to Au substrates and their surrounding media has centered on ionic binding,<sup>1–4</sup>

covalent bonding,<sup>5,6</sup> hydrogen bonding,<sup>7–9</sup> acid/base interactions,<sup>8,10,11</sup> complexation phenomena,<sup>12</sup> effect of applied potential on structure,<sup>13</sup> and the effect of solvent.<sup>14</sup> Two groups have published studies that correlate the depth of functional groups within two-component SAMs to their reactivity.<sup>12,14</sup> In this paper, we use single-component MBA monolayers because the reactive carboxylic acid groups reside at varying depths and in structurally distinct environments depending upon the isomer. Moreover, since the SAMs are formed from a single component, it is reasonably straightforward to estimate their structure. This is in sharp contrast to multicomponent SAMs, which

(1) Sun, L.; Johnson, B.; Wade, T.; Crooks, R. M. *J. Phys. Chem.* **1990**, *94*, 8869.

(2) Tarlov, M. J.; Bowden, E. F. *J. Am. Chem. Soc.* **1991**, *113*, 1847.

(3) Collinson, M.; Bowden, E. F.; Tarlov, M. J. *Langmuir* **1992**, *8*, 1247.

(4) Jones, T. A.; Perez, G. P.; Johnson, B. J.; Crooks, R. M. *Langmuir* **1995**, *11*, 1318.

(5) Duevel, R. V.; Corn, R. M. *Anal. Chem.* **1992**, *64*, 337.

(6) Sun, L.; Thomas, R. C.; Crooks, R. M.; Ricco, A. J. *J. Am. Chem. Soc.* **1991**, *113*, 8550.

(7) Kepley, L. J.; Crooks, R. M.; Ricco, A. J. *Anal. Chem.* **1992**, *64*, 3194.

(8) Roush, J. A.; Thacker, D. L.; Anderson, M. R. *Langmuir* **1994**, *10*, 1642.

(9) Sun, L.; Kepley, L. J.; Crooks, R. M. *Langmuir* **1992**, *8*, 2101.

(10) Bryant, M. A.; Crooks, R. M. *Langmuir* **1993**, *9*, 385.

(11) Sun, L.; Crooks, R. M.; Ricco, A. J. *Langmuir* **1993**, *9*, 1775.

(12) Rubinstein, I.; Steinberg, S.; Tor, Y.; Shanzler, A.; Sagiv, J. *Nature* **1988**, *332*, 426.

(13) Anderson, M. R.; Gatin, M. *Langmuir* **1994**, *10*, 1638.

(14) Rowe, G. K.; Creager, S. E. *Langmuir* **1991**, *7*, 2307.

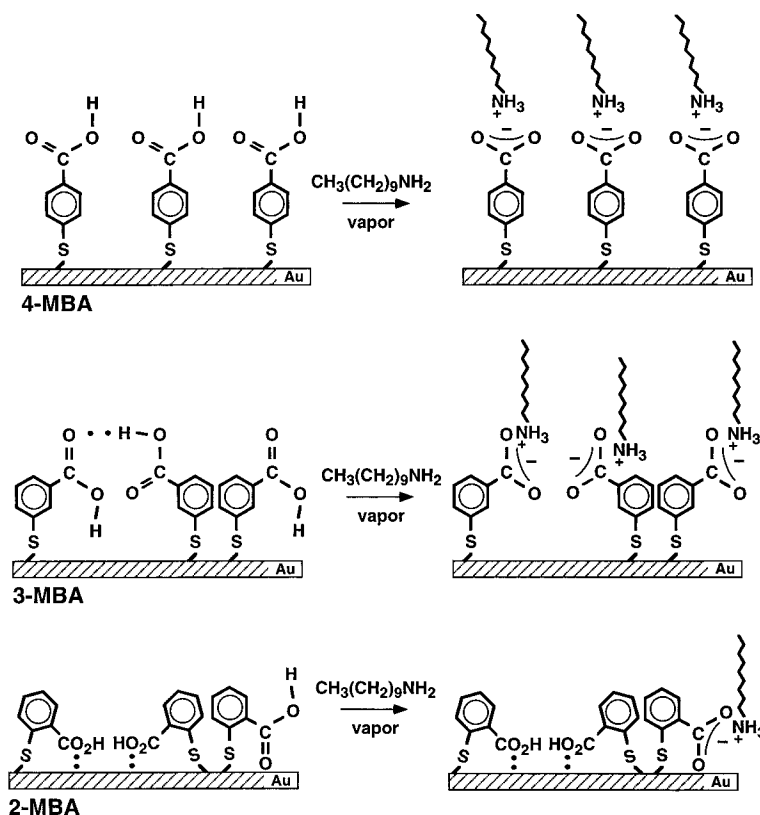
\* Authors to whom correspondence should be addressed.

† e-mail, crooks@chemvx.tamu.edu; fax, 409-845-1399; voice, 409-845-5629.

‡ e-mail, ajricco@sandia.gov; fax, 505-844-1198; voice, 505-844-1405.

⊗ Abstract published in *Advance ACS Abstracts*, March 15, 1996.

Scheme 1



appear to form domains that are just beginning to be understood.<sup>15</sup>

We chose Fourier transform infrared external reflection spectroscopy (FTIR-ERS) to monitor the interaction between the MBA SAMs and decylamine, because it provides chemical information about the surface-confined reaction products. We couple these spectroscopic data with nanogravimetry based on thickness-shear-mode resonators (TSMRs), which provide quantitative information about the mass of the reaction products.<sup>16</sup> Finally, we show that X-ray photoelectron spectroscopy (XPS) qualitatively corroborates results obtained from FTIR-ERS and nanogravimetry.

### Experimental Section

We obtained 4- and 3-MBA from Toronto Research Chemicals, Inc. (Ontario, Canada), and 2-MBA from Aldrich Chemical Co. (Milwaukee, WI) and purified all isomers by sublimation. Au surfaces for FTIR-ERS and XPS were prepared by electron-beam deposition of 100 Å of Cr followed by 2000 Å of Au onto polished Si(100) wafers. Wafers were diced into  $1 \times 3$  cm pieces and, immediately prior to derivitization, cleaned using a low-energy Ar plasma cleaner (Harrick Scientific Model PDC-32G, Ossining, NY) for 30 s, then immersed in 1 mM ethanolic solutions of the appropriate MBA isomer for  $24 \pm 2$  h. Prior to analysis by FTIR-ERS, each substrate was soaked in either  $\text{pH} = 6.2 \pm 0.1$  deionized water, a  $\text{pH} = 3$  HCl solution, or a  $\text{pH} = 8.5$  KOH solution for 10 min and then dried under flowing  $\text{N}_2$ . Dilute acid and base solutions were made from concentrated HCl (Spectrum Chemical,

Gardena, CA) and solid KOH (Mallinckrodt, Paris, KY), respectively, mixed with deionized water.

FTIR-ERS data were obtained using a  $\text{N}_2$ -purged Digilab FTS-40 FTIR spectrometer (Bio-Rad, Cambridge, MA) equipped with a Seagull variable-angle reflection accessory (Harrick Scientific). The p-polarized light was focused on the Au surface at an  $85^\circ$  angle of incidence with respect to the surface normal, and the reflected beam was detected by a liquid- $\text{N}_2$ -cooled MCT detector. Spectra of the MBA monolayers were referenced to a nominally naked Au substrate, using the following instrumental parameters: triangular apodization,  $4 \text{ cm}^{-1}$  resolution, and 256 scans. Real-time difference spectra of the MBA monolayers were obtained during and after dosing using an unreacted MBA monolayer as the reference substrate under the following conditions: triangular apodization,  $4 \text{ cm}^{-1}$  resolution, and 64 scans. The surface was dosed with a 50%-of-saturation decylamine vapor at a flow rate of 0.5 L/min using an *in-situ* technique developed in our laboratory.<sup>17,18</sup> We acquired subtraction spectra using Bio-Rad Idris-based software, which enables mathematical subtraction of one absorbance spectrum from another taken under the same instrumental conditions.

All of the TSMR experiments utilize 9-MHz AT-cut quartz devices (Kyushu Dentsu Co. Ltd., Omura City, Japan). The electrodes consist of a 2000 Å Au layer deposited over a 150 Å Ni adhesion layer. We cleaned the Au electrodes and modified them with SAMs exactly as described for the FTIR-ERS and XPS substrates. The oscillator circuit for TSMR experiments consists of a TSMR, a 5-V dc power supply (Newark Model 89F1268, Chicago, IL), a frequency counter (Hewlett-Packard Model 5384A, Santa Rosa, CA), an oscillator circuit (Leybold Inficon Model 013-001, Syracuse, NY), and a custom-built frequency filter,<sup>19</sup> arranged in a configuration described elsewhere.<sup>19</sup> Two stainless-steel flow cells each housed one TSMR device. The decylamine dosing conditions were identical to those used for the spectroscopic experiments.

(15) Stranick, S. J.; Parikh, A. N.; Tao, Y.-T.; Allara, D. L.; Weiss, P. S. *J. Phys. Chem.* **1994**, *98*, 7636.

(16) Changes in TSM wave velocity and amplitude are affected by factors other than simple mass change. Since the films used here are acoustically thin (See: Ricco, A. J. *Electrochem. Soc. Interface* **1994**, *3*, 38), the principal obstacle to accurate mass measurements will result from changes in the viscoelastic properties of the film (See Martin, S. J.; Frye, G. C.; Senturia, S. *Anal. Chem.* **1994**, *66*, 2201). For the results presented in this paper we believe errors resulting from this effect are minimal, but we are studying the phenomenon in depth at the present time.

(17) Xu, C.; Sun, L.; Kepley, L. J.; Crooks, R. M.; Ricco, A. J. *Anal. Chem.* **1993**, *65*, 2102.

(18) Crooks, R. M.; Sun, L.; Xu, C.; Hill, S. L.; Ricco, A. J. *Spectroscopy* **1992**, *7*, 2.

(19) Yang, H. C.; Dermody, D. L.; Xu, C.; Ricco, A. J.; Crooks, R. M. *Langmuir* **1996**, *12*, 726.

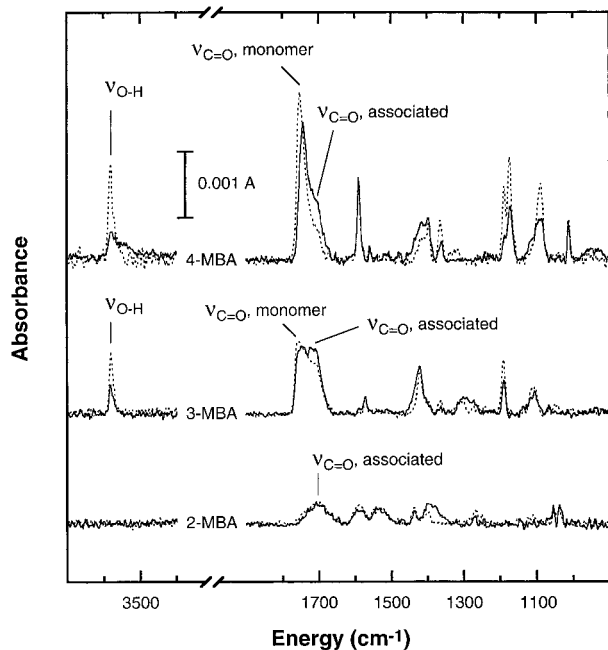


**Figure 1.** FTIR-ERS spectra of 4-, 3-, and 2-MBA SAMs. The dashed lines indicate spectra obtained within 15 min of removal from MBA/ethanol solutions, and the solid lines indicate spectra obtained after aging the SAMs in H<sub>2</sub>O- and CO<sub>2</sub>-free air for 3 h at room temperature.

The TSMR surface-coverage calculations include a surface-roughness factor of  $1.2 \pm 0.2$ . This value was measured by selecting representative TSMRs from each batch supplied by the vendor, and exposing them, after cleaning, to 25%-of-saturation *n*-heptanethiol vapor mixed down in N<sub>2</sub>. From previous experiments, we know that *n*-heptanethiol adsorbs irreversibly as a full monolayer onto Au surfaces from the vapor phase.<sup>20</sup> By comparison of the measured to the theoretical (0.78 nmol/cm<sup>2</sup> for an atomically flat, defect-free Au(111) surface)<sup>19</sup> SAM coverage, an estimate of the surface-roughness factor is obtained. Each of the TSMR experiments was repeated several times to determine the extent of variability in the measurements. The TSMR data exhibit a maximum standard deviation of 0.06 (expressed as fractional coverage), or an absolute maximum standard deviation of 7 ng/cm<sup>2</sup>.

We collected XPS data using a Perkin-Elmer Model 5500 photoelectron spectrometer outfitted with a Mg K $\alpha$  source ( $E = 1253.6$  eV, 400 W). The analyzer was oriented at a photoelectron take-off angle of 45° from the surface normal. Spectra of C, O, and S were obtained using a 29.35 eV pass energy and a 1 × 3 mm analyzer aperture. The pressure in the chamber during analysis was approximately  $2 \times 10^{-8}$  mmHg.

## Results and Discussion

FTIR-ERS spectra of 4-, 3-, and 2-MBA SAMs are shown in Figure 1. The dashed lines represent spectra of N<sub>2</sub>-dried SAMs obtained immediately after removal from pH = 6.2 deionized water, and the solid lines are spectra obtained after the SAMs were exposed to a H<sub>2</sub>O- and CO<sub>2</sub>-free air purge for ~3 h. The most striking feature of these spectra is the decrease in absorbance and increase in width for most bands as the proximity of the carboxylic acid group to the Au surface increases. This trend is consistent with previous observations of the influence metals have upon the vibrational spectra of benzoic acids. The effect arises from a redistribution of electronic charge in the aromatic ring upon either complexation with a metal ion (metal benzoates)<sup>21,22</sup> or contact between the acid group

and metal oxide<sup>23</sup> or metal surfaces.<sup>24</sup> In previous studies, the magnitudes of such spectral changes were correlated to a decrease in the oxidation state and electronegativity of the metal and an increase in its atomic mass.<sup>21–23</sup> Since these effects require significant metal/carboxyl group interaction, it is not surprising that the spectral features of 2-MBA are so distinctly different from those of 3-MBA, and still more different from those of 4-MBA.

A second striking feature of the spectra in Figure 1 is the changes that occur in the monolayers after a 3-h exposure to H<sub>2</sub>O- and CO<sub>2</sub>-free air. These changes, which are most dramatic for 4-MBA, less striking in the 3-MBA spectrum, and unremarkable in the spectrum of 2-MBA, are related to a slow structural reorganization of the monolayer (*vide infra*).

Table 1 lists peak assignments for the freshly prepared, unaged MBA SAMs (dashed-line spectra, Figure 1). The carboxylic acid group modes are most revealing with regard to the structure of the MBA SAMs. The 4-MBA spectrum shows a sharp O–H stretch ( $\nu_{O-H}$ ) at 3579 cm<sup>-1</sup> and a pronounced C=O stretch ( $\nu_{C=O}$ ) at 1751 cm<sup>-1</sup> with a shoulder centered at approximately 1709 cm<sup>-1</sup>. The band at 1397 cm<sup>-1</sup> is located in the correct position for a carboxylate symmetric stretch ( $\nu_{s,CO_2}$ ), although this band could also originate from a ring mode.<sup>21–23,25,26</sup> The  $\nu_{O-H}$  and  $\nu_{C=O}$  modes occur at vibrational frequencies corresponding to monomeric carboxylic acid groups<sup>27–37</sup> and denote an absence of intramonomer hydrogen bonding between adjacent 4-MBA molecules. However, the small low-energy shoulder on the carbonyl peak indicates that some 4-MBA molecules do participate in lateral hydrogen bonding<sup>11</sup> but that this is not the predominant conformation. The absorbance of the band at 1397 cm<sup>-1</sup> is very small relative to that of a fully deprotonated 4-MBA SAM (*vide infra*); therefore, even if this band does correspond to  $\nu_{s,CO_2}$ , the monolayer is almost completely protonated.

The 4-MBA spectrum obtained after aging the SAM for 3 h in H<sub>2</sub>O- and CO<sub>2</sub>-free air (solid line, Figure 1) reveals three noteworthy changes. First there is a lowering of the monomeric  $\nu_{C=O}$  peak energy and redistribution of the  $\nu_{C=O}$  peak toward the associated, hydrogen-bonded state. This change is accompanied by a downward energy shift and broadening of the  $\nu_{O-H}$  peak. Second, there is a decrease in the intensities of several peaks in the region below 1400 cm<sup>-1</sup>. Third, we observe a slight intensity increase and broadening of the 1397 cm<sup>-1</sup> band. The first change is strong evidence that the SAM undergoes a

(23) Koustaal, C. A.; Ponec, V. *Appl. Surf. Sci.* **1993**, *70/71*, 206.

(24) Stern, D. A.; Laguren-Davidson, L.; Frank, D. G.; Gui, J. Y.; Lin, C.-H.; Lu, F.; Salaita, G. N.; Walton, N.; Zapfen, D. C.; Hubbard, A. T. *J. Am. Chem. Soc.* **1989**, *111*, 877.

(25) Green, J. H. S. *Spectrochim. Acta* **1977**, *33A*, 575.

(26) Kondo, J.; Ding, N.; Maruya, K.; Domen, K.; Yokoyama, T.; Fujita, N.; Maki, T. *Bull. Chem. Soc. Jpn.* **1993**, *66*, 3085.

(27) Colthup, N. B.; Daly, L. H.; Wiberley, S. E. *Introduction to Infrared and Raman Spectroscopy*, 3rd ed.; Academic: San Diego, CA, 1990.

(28) Lin-Vien, D.; Colthup, N. B.; Fately, W. G.; Grasselli, J. G. *Infrared and Raman Characteristic Frequencies of Organic Molecules*; Academic: San Diego, CA, 1991.

(29) Kato, T.; Chihiro, J.; Kaneuchi, F.; Uryu, T. *Bull. Chem. Soc. Jpn.* **1993**, *66*, 3581.

(30) Krygowski, T. M.; Wiedcowski, T.; Sokolowska, A. *Croat. Chem. Acta* **1984**, *57*, 229.

(31) Bellamy, L. J.; Pace, R. J. *Spectrochim. Acta* **1963**, *19*, 435.

(32) Mori, N.; Kaido, S.; Suzuki, K.; Nakamura, M.; Tsuzuki, Y. *Bull. Chem. Soc. Jpn.* **1971**, *44*, 1858.

(33) Brooks, C. J. W.; Eglinton, G.; Morman, J. F. *Spectrochim. Acta* **1961**, *13*, 106.

(34) Creager, S. E.; Steiger, C. M. *Langmuir* **1995**, *11*, 1852.

(35) Brycki, B.; Brzezinski, B.; Grech, E. *J. Chem. Soc., Perkin Trans. 2* **1991**, 1209.

(36) Bueno, W. A.; Morgado, F. *Spectrochim. Acta* **1993**, *49A*, 249.

(37) Takenaka, S.; Kondo, K.; Tokura, N. *J. Chem. Soc. Perkin Trans. 2* **1974**, 1749.

(20) Thomas, R. C.; Sun, L.; Crooks, R. M.; Ricco, A. J. *Langmuir* **1991**, *7*, 620.

(21) Lewandowski, W. *Can. J. Spectrosc.* **1987**, *32*, 41.

(22) Lewandowski, W. *J. Mol. Struct.* **1983**, *101*, 93.

**Table 1. Vibrational Assignments for FTIR-ERS Spectra of Surface-Confined MBA Isomers<sup>a</sup>**

4-MBA		3-MBA		2-MBA	
energy (cm <sup>-1</sup> )	assignment	energy (cm <sup>-1</sup> )	assignment	energy (cm <sup>-1</sup> )	assignment
3579 s	$\nu_{\text{O-H}}$	3580 m	$\nu_{\text{O-H}}$	3066 vw	$\nu_{\text{C-C}}$ (2, 20a)
1751 vs; 1709 sh	$\nu_{\text{C=O}}$	1750 s; 1708 sh	$\nu_{\text{C=O}}$	1720 w	$\nu_{\text{C=O}}$
1589 s	$\nu_{\text{C-C}}$ (8a)	1567 vw	$\nu_{\text{C-C}}$ (8a)	1690 w	$\nu_{\text{C=O}}$
1560 vw	$\nu_{\text{C-C}}$ (8b)	1417 m	$\nu_{\text{C-C}}$ (19a)	1583 w	$\nu_{\text{C-C}}$ (8a, 8b)
1419 w	$\nu_{\text{C-C}}$ (19b) or $\nu_{\text{s,CO}_2^-}$	1360 vw	$\beta_{\text{O-H}}$	1529 w	$\nu_{\text{C-C}}$ (19b)
1397 m	$\nu_{\text{s,CO}_2^-}$	1301 vw	$\beta_{\text{C-H}}$ (14)	1429 vw	$\nu_{\text{C-C}}$ (19a)
1365 m	$\beta_{\text{O-H}}$ or $\beta_{\text{C-H}}$ (14)	1188 m	$\beta_{\text{C-H}}$ (9b, 13) or $\nu_{\text{C-O}}$	1393 w	$\nu_{\text{s,CO}_2^-}$
1189 s	$\beta_{\text{C-H}}$ (9a) or $\nu_{\text{C-O}}$	1110 w	$\beta_{\text{C-H}}$ (18a) or $\nu_{\text{C-O}}$	1048 w	$\beta_{\text{C-H}}$ (1, 18b)
1175 s	$\beta_{\text{C-H}}$ (9a) or $\nu_{\text{C-O}}$			1035 w	$\beta_{\text{C-H}}$ (1, 18b)
1090 s	$\beta_{\text{C-H}}$ (18b) or $\nu_{\text{C-O}}$				
1014 m	$\beta_{\text{C-H}}$ (18a)				

<sup>a</sup> Key: vs, s, m, w, vw: very strong, strong, medium, weak, very weak; sh, shoulder. Numbers in parentheses refer to the normal vibrations of the benzene ring for the  $C_{2v}$  point group (in the case of 4-MBA) and the  $C_s$  point group (in the case of 3- and 2-MBA).<sup>40</sup>

gradual surface reordering toward a more highly associated state. Electronic changes connected to this reordering could also affect the substituent-sensitive spectral region below 1400 cm<sup>-1</sup>, which would account for the decreases in peak intensities in that spectral region. This rationale may also apply to the increase in the 1397 cm<sup>-1</sup> band intensity if it originates from a ring mode. Alternatively, this band might also arise from carboxylate species in the SAM ( $\nu_{\text{s,CO}_2^-}$ , Table 1 and *vide infra*). We view the latter possibility as unlikely for want of further confirming evidence or a probable mechanism.

The spectrum of the freshly prepared 3-MBA SAM (dashed line, Figure 1) reveals a  $\nu_{\text{O-H}}$  band at 3580 cm<sup>-1</sup> and a  $\nu_{\text{C=O}}$  band at 1750 cm<sup>-1</sup> with a shoulder centered at 1708 cm<sup>-1</sup>. The low-energy shoulder on the 1417 cm<sup>-1</sup> peak could result from  $\nu_{\text{s,CO}_2^-}$ , but the magnitude of this peak is insignificant compared to that of a fully deprotonated 3-MBA monolayer, indicating that the SAM is completely, or nearly completely, protonated (*vide infra*). The percentage of the  $\nu_{\text{C=O}}$  peak present at 1708 cm<sup>-1</sup> is much larger in the 3-MBA SAM than in the 4-MBA SAM. Likewise, the monomeric  $\nu_{\text{O-H}}$  peak at 3580 cm<sup>-1</sup> is significantly smaller than that of 4-MBA. From these observations we conclude that the extent of intramonolayer hydrogen bonding is greater for 3-MBA SAMs than for 4-MBA SAMs, and from the relative distribution of the  $\nu_{\text{C=O}}$  band between 1750 and 1708 cm<sup>-1</sup> we conclude that the ratio of associated and monomeric carboxylic acid groups in the 3-MBA SAM is near 1.

The 3-MBA SAM can assemble with the carboxyl groups facing either toward or away from each other; the former geometry is represented by the left and middle molecules in the center frame of Scheme 1, and the latter geometry is represented by the right and middle molecules. Of course, since the SAM surfaces are two-dimensional, alternative intermediate geometries are also possible. CPK models verify that carboxyl groups facing "toward" each other are close enough to hydrogen bond ( $\sim 2$  Å).<sup>30,33,38</sup> We anticipate an approximately equal distribution of laterally hydrogen-bonded acid dimers and non-hydrogen bonded monomers if the monolayer self-assembles with an equal probability of carboxylic acid groups facing toward and away from each other and if the 3-MBA molecules are not free to rotate about their C-S bond axes.<sup>11</sup> Although the spectrum of the freshly prepared 3-MBA SAM indicates a slight excess of monomeric acid groups compared to the hydrogen-bonded form, the spectrum of 3-MBA obtained after aging 3 h in H<sub>2</sub>O- and CO<sub>2</sub>-free air (solid line, Figure 1) shows that there are two distinct  $\nu_{\text{C=O}}$  bands of equal intensity at 1739 and 1710 cm<sup>-1</sup>.

After 3 h, there are changes in the 3-MBA SAM that are similar to those observed for the 4-MBA SAM. The decrease in the 3-MBA  $\nu_{\text{O-H}}$  band at 3580 cm<sup>-1</sup> and changes in intensity of bands in the low-energy region of the spectrum result from the transformation of monomeric acid groups into hydrogen-bonded acid groups. Both 4- and 3-MBA SAMs also display a 5–10 cm<sup>-1</sup> downward energy shift of the monomeric  $\nu_{\text{C=O}}$  band after 3 h in H<sub>2</sub>O- and CO<sub>2</sub>-free air.

The spectrum of 2-MBA reveals a broad, weak  $\nu_{\text{C=O}}$  band centered at 1720 cm<sup>-1</sup> and ranging from about 1740 to 1655 cm<sup>-1</sup>. We have obtained spectra of several independently prepared 2-MBA monolayers, and in some of them this band has a bimodal appearance with broad overlapping peaks at approximately 1720 and 1675 cm<sup>-1</sup>. Like 3-MBA, the 2-MBA SAM should have an equal distribution of laterally hydrogen-bonded and non-hydrogen-bonded acid groups. However, since these bands are broad and indistinct, it is difficult to interpret them with confidence. As previously stated, benzoic acid compounds contacting a metal surface may exhibit weakened or altered spectral features resulting from the redistribution of electronic charge in the aromatic ring. Flattening and broadening of the 2-MBA  $\nu_{\text{C=O}}$  band may result from back donation of electrons from Au to oxygen;<sup>24</sup> in organometallic compounds this type of behavior results in decreasing acidity for CO ligands and a lowering of the carbonyl spectral band energy.<sup>39</sup> Importantly, we do not observe a 2-MBA  $\nu_{\text{O-H}}$  peak at 3579 cm<sup>-1</sup>, indicating that all or most of the 2-MBA carboxyl groups in the SAM are not carboxylic acid "monomers". This observation is in accord with the diminished magnitude and low-energy position of the broad 2-MBA  $\nu_{\text{C=O}}$  band and our conclusion that the 2-MBA carboxyl groups are interacting with the surface.

The spectrum of the freshly prepared 2-MBA SAM (dashed line, Figure 1) has a very weak band at 1393 cm<sup>-1</sup>, which is the expected position for the  $\nu_{\text{s,CO}_2^-}$  band. An increase in this band is the only significant change in the spectrum of 2-MBA obtained 3 h later (solid line, Figure 1). Thus there is no strong evidence for the type of reorganization observed for the 3- and 4-MBA SAMs.

Aromatic ring modes for the MBA monolayers are somewhat difficult to assign because of the very low absorbances, shifts in peak absorbance and energy resulting from surface adsorption and interactions of the adsorbed species with the substrate and nearby adsorbates, and the effect of the carboxyl-group ring substituent upon some bands that may result in energy shifts of up

(38) Vinogradov, S. N.; Linnell, R. H. *Hydrogen Bonding*; Van Nostrand Reinhold Co.: New York, 1971.

(39) Cotton, F. A.; Wilkinson, G. *Advanced Inorganic Chemistry*, 4th ed.; Wiley: New York, 1980.

to  $200\text{ cm}^{-1}$ .<sup>27,28,40</sup> With these caveats in mind, ring-mode assignments are given in Table 1 for the spectra of the MBA SAMs shown in Figure 1. These assignments are based on comparisons with literature data<sup>27,28,40</sup> and spectra of related benzene derivatives.<sup>25,26,41–43</sup> Generally, bands located above  $1400\text{ cm}^{-1}$  are ring-quadrant and semicircle stretches ( $\nu_{C-C}$ ), bands between  $1400$  and  $900\text{ cm}^{-1}$  are substituent-sensitive wagging modes ( $\beta_{C-H}$ ), and bands below  $900\text{ cm}^{-1}$  are out-of-plane bends ( $\nu_{C-H}$ ).

Assigning bands in the spectral region around  $1400\text{ cm}^{-1}$  is problematic in compounds containing both aromatic rings and carboxyl groups since this frequency is characteristic of the  $\nu_{s,CO_2^-}$  band as well as ring semicircle stretches ( $\nu_{C-C}$  19a and b, see Table 1). Additionally, bands in the  $1400 \pm 30\text{ cm}^{-1}$  region have been assigned to the  $\beta_{O-H}$  mode<sup>44</sup> of the carboxylic acid group.<sup>5,34</sup> The  $\beta_{O-H}$  mode is one of the weaker carboxylic acid modes, and hence it seems more likely that peaks in this region result from  $\nu_{s,CO_2^-}$  and/or the  $\nu_{C-C}$  aromatic band. To better understand the acid–base behavior of these monolayers, 4-, 3-, and 2-MBA SAMs were soaked in a pH = 3 HCl solution for 10 min, dried with flowing  $N_2$ , and then analyzed by FTIR-ERS within 15 min of drying. Next the monolayers were soaked in a pH = 8.5 KOH solution for an additional 10 min, dried with flowing  $N_2$ , and again analyzed by FTIR-ERS.

The upper two spectra in each frame of Figure 2 illustrate the results of this experiment. Clearly, large changes in  $\nu_{C=O}$  result from changing the pH of the SAM environment from acidic to basic. In the acidic environment, each monolayer has a fully developed  $\nu_{C=O}$  peak and, for those spectra displaying monomeric carbonyl bands at  $\nu_{C=O} = 1740\text{--}50\text{ cm}^{-1}$ , a fully developed  $\nu_{O-H}$  stretch, all of which indicate the presence of protonated carboxyl groups. Correspondingly, in the basic environment, each monolayer lacks a significant  $\nu_{C=O}$  or  $\nu_{O-H}$  peak and has a well-developed  $\nu_{s,CO_2^-}$  peak, which indicates deprotonation of the acid. At pH = 3 and pH = 8.5, the 3- and 4-MBA SAMs appear to be fully protonated and fully deprotonated, respectively. In contrast, the 2-MBA SAM appears to have small carboxylate features even at pH = 3 and a small carboxylic acid feature at pH = 8.5.

The bottom spectra in Figure 2 are subtraction spectra, and they demonstrate the changes undergone by each monolayer upon deprotonation. These subtraction spectra display no negative peaks from the base-induced disappearance of the associated  $\beta_{O-H}$  mode (typical range is  $1440\text{--}1395\text{ cm}^{-1}$ ), but there is a small negative band at  $1365\text{ cm}^{-1}$  in the pH = 3 spectrum of 4-MBA and a very weak band at  $1360\text{ cm}^{-1}$  in the pH = 3 spectrum of 3-MBA that may result from the base-induced disappearance of the monomeric  $\beta_{O-H}$  mode (typical range is  $1280\text{--}1385\text{ cm}^{-1}$ ).<sup>27,28,40</sup> We conclude that bands in the region of  $1400 \pm 20\text{ cm}^{-1}$  result from either  $\nu_{s,CO_2^-}$  or substituent-sensitive  $\nu_{C-C}$  rather than  $\beta_{O-H}$ .<sup>5,34</sup>

FTIR-ERS single-beam spectra of MBA monolayers were obtained in real time during and after dosing with vapor-phase decylamine and referenced to single-beam spectra of the monolayers obtained prior to decylamine

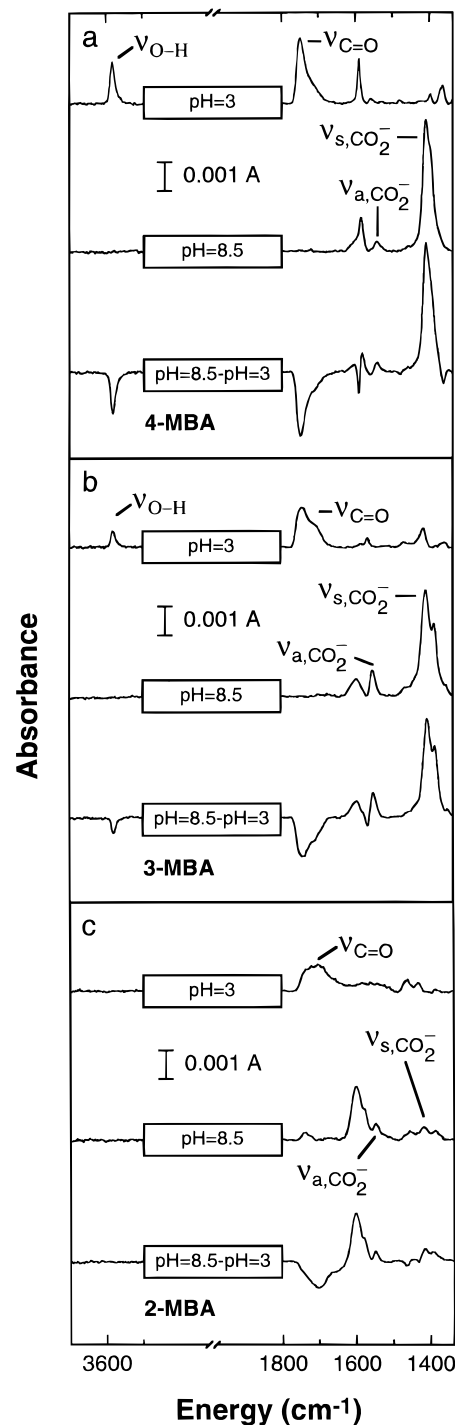


**Figure 2.** FTIR-ERS spectra of (a) 4-MBA, (b) 3-MBA, and (c) 2-MBA SAMs obtained after soaking in pH = 3 solutions (top) and pH = 8.5 solutions (middle). Subtraction spectra (bottom) illustrate the spectral changes that occur upon deprotonation of the MBA monolayers.

exposure. Parts a–c of Figure 3 show the resultant difference spectra of 4-, 3-, and 2-MBA SAMs, respectively, after equilibrating the monolayers in the flow cell under a pure  $N_2$  purge for 35 min, dosing for 20 min with decylamine, and then purging with pure  $N_2$  for the times indicated in the figure. The peak assignments for the bands in Figure 3 are given in Table 2. Decylamine aliphatic C–H stretches ( $\nu_{a,C-H(CH_3)}$ ,  $\nu_{a,C-H(CH_2)}$ ,  $\nu_{s,C-H(CH_3)}$ ,  $\nu_{s,C-H(CH_2)}$ ) between  $2800$  and  $3000\text{ cm}^{-1}$  appear in all spectra. The intensity of the  $\nu_{C-H}$  peaks is strongest during dosing since vapor-phase decylamine is in the flow-cell headspace and perhaps loosely physisorbed to the MBA SAMs. At the onset of  $N_2$  purging, these peaks decrease

(40) Varsányi, G. *Assignments for Vibrational Spectra of Seven Hundred Benzene Derivatives*; Wiley: New York, 1974.

(41) Ansari, A. K.; Verma, P. K. *Indian J. Pure Appl. Phys.* **1979**, *17*, 632.

(42) Sánchez de la Blanca, E.; Núñez, J. L.; Martínez, P. *J. Mol. Struc.* **1986**, *142*, 45.

(43) González-Sánchez, F. *Spectrochim. Acta* **1958**, *12*, 17.

(44) The bands  $\beta_{O-H}$  and  $\nu_{C-O}$  are closely coupled and hence may be juxtaposed in some literature. Also,  $\beta_{O-H}$  may be referred to as  $\beta_{O-H} + \nu_{C-O}$  and  $\nu_{C-O}$  may be referred to as  $\nu_{C-O} + \beta_{O-H}$ . See refs 5, 27, 34, and 43.

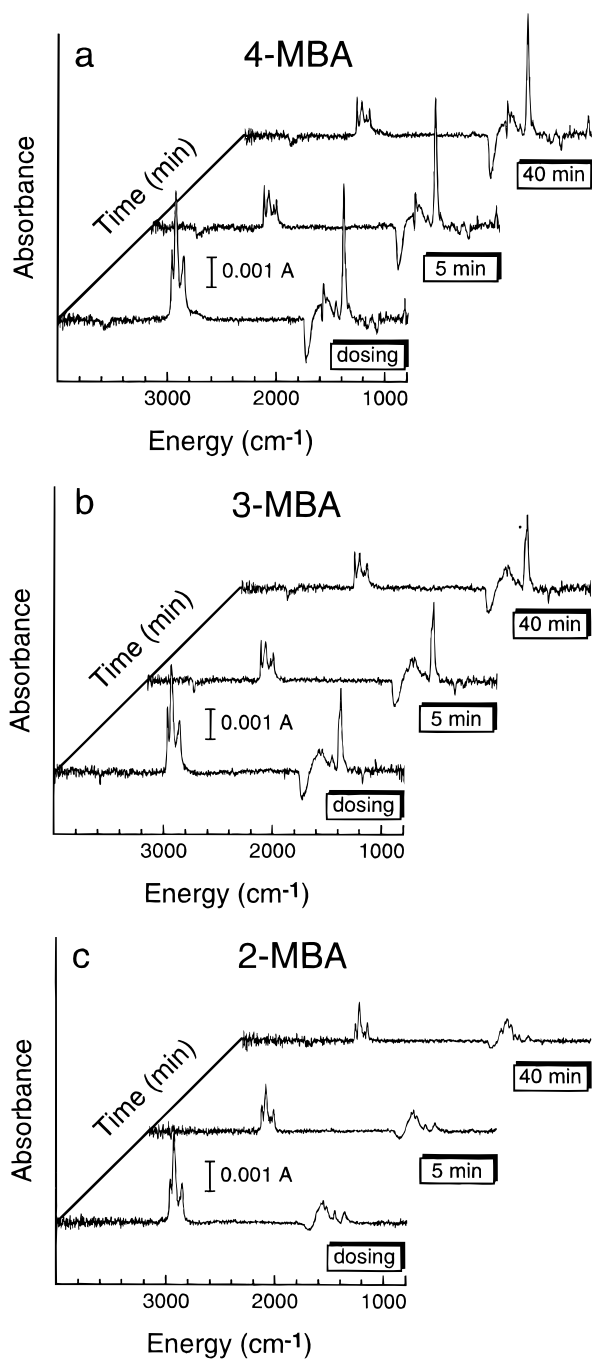


**Figure 3.** Time-resolved difference spectra of (a) 4-MBA, (b) 3-MBA, and (c) 2-MBA SAMs during and after exposure to decylamine vapor. The bottom spectrum in each panel was obtained at steady state during dosing and includes contributions from vapor-phase decylamine in the cell headspace. The top two spectra in each panel were obtained after purging the cell with pure  $N_2$  for the times indicated.

in intensity as vapor-phase and physisorbed decylamine are cleared from the flow cell. Control experiments performed using methyl-terminated SAMs indicate that after 40 min of  $N_2$  purging only decylamine specifically adsorbed to the MBA SAMs remains.<sup>11</sup> For 4- and 3-MBA SAMs, the intensities of  $\nu_{a,C-H(CH_2)}$  and  $\nu_{a,C-H(CH_3)}$  are approximately equal, whereas for the 2-MBA SAM  $\nu_{a,C-H(CH_2)}$  is much larger than  $\nu_{a,C-H(CH_3)}$ . Since intercalation of decylamine into the 2-MBA monolayer is presumably a prerequisite for proton transfer, this observation may reflect an orientational constraint imposed by the mechanism of intercalation. The orientation of adsorbed decylamine, reflected by the relative intensities of the  $\nu_{C-H}$  bands is also dependent upon SAM age and structure.<sup>19</sup>

Parts a and b of Figure 3 show growth of very strong  $\nu_{s,CO_2^-}$  bands at 1397 and 1384  $cm^{-1}$ , respectively, and concomitant formation of negative  $\nu_{C=O}$  and  $\nu_{O-H}$  peaks. These bands confirm proton transfer from MBA to decylamine. There is also a weak  $\nu_{a,CO_2^-}$  stretch at  $\sim 1550$   $cm^{-1}$ , which in bulk phase is normally of greater intensity than  $\nu_{s,CO_2^-}$ . For 4-MBA oriented with the ring plane nearly normal to the surface, there should be a strong  $\nu_{s,CO_2^-}$  band and little absorbance arising from  $\nu_{a,CO_2^-}$  because of the IR surface-selection rule.<sup>45,46</sup> This orientation for 4-MBA is consistent with previous findings for terephthalic acid adsorbed to alumina<sup>47</sup> and for carboxylic acid-substituted pyridines bound to Pt through the ring N.<sup>24</sup> On the basis of orientational effects only, it might be anticipated that the  $\nu_{s,CO_2^-}$  bands for 3-MBA and 2-MBA would be similar in magnitude, but attenuated relative to 4-MBA. However, all the proton-transfer-related bands, particularly  $\nu_{s,CO_2^-}$ , are very strong for 4-MBA, less intense for 3-MBA, and very weak for 2-MBA. This trend correlates strongly with the reactivity of these monolayers, which we determined using TSMRs, and therefore we ascribe the spectral changes to structurally-imposed differences in reactivity.

The shape of the  $\nu_{s,CO_2^-}$  band in Figure 3b warrants comment. Prior to dosing, the spectrum of the 3-MBA SAM reveals a monomeric carbonyl peak with a large shoulder spanning the energy range characteristic of associated carboxylic acid groups. If the 3-MBA monolayer is allowed to age for 3 h in  $H_2O$ - and  $CO_2$ -free air, two distinct centroids emerge, confirming that there are two distinct environments for the carboxylic acid groups (Figure 1). After reaction with decylamine, the  $\nu_{C=O}$  band becomes negative and is replaced by two new  $\nu_{s,CO_2^-}$  bands at 1384 and 1403  $cm^{-1}$ . The presence of two distinct  $\nu_{s,CO_2^-}$  peaks attests to the persistence of these two distinct environments in the 3-MBA monolayer. Unlike 3-MBA, the spectrum of 4-MBA prior to dosing indicates predominantly monomeric acid groups, and after exposure to decylamine there is a single  $\nu_{s,CO_2^-}$  peak accompanied by an indistinct low-energy shoulder.

The spectra shown in Figure 2 and Figure 3 illustrate the sensitivity of the ring structure to carboxyl-group changes. The spectra in Figure 2 show that notable changes occur in the quadrant stretch region ( $\nu_{C-C}$ , 8a and 8b, see Tables 1 and 2) of all MBA SAMs upon deprotonation. The difference spectra in Figure 3 reflect similar changes resulting from MBA proton transfer to decylamine. In 4-MBA, loss of a proton results in a change in benzene-ring electron density which produces a new band that has the appearance of a first-derivative peak (1582–1591  $cm^{-1}$ ). This “first-derivative” structure is superimposed upon a broad band that is attributable to  $\nu_{N-H(NH_3^+)}$  and  $\nu_{a,CO_2^-}$ .<sup>48</sup> We have examined proton-transfer reactions involving aliphatic surface-confined species that yield similar difference spectra except that no such “first-derivative” feature is apparent.<sup>19</sup> This shift in energy upon proton transfer is obvious in the 4-MBA difference spectra, less pronounced for 3-MBA, and not apparent in the 2-MBA difference spectra. While the 4-MBA quadrant stretch region is markedly more developed than that of 3- and 2-MBA in Figure 1, upon deprotonation (Figure 2) the 4-MBA quadrant stretch loses intensity and that of 3-MBA and particularly 2-MBA gain intensity. Changes in aromatic spectral bands upon formation of negatively

(45) Porter, M. D. *Anal. Chem.* **1988**, *60*, 1143A.

(46) Groff, R. P. *J. Catal.* **1983**, *79*, 259.

(47) Ogawa, H. *J. Phys. Org. Chem.* **1991**, *4*, 346.

(48) The existence of aryl-carboxyl group bands in the 1600–1700  $cm^{-1}$  range, which result from  $CO_2H$  and  $CO_2^-$  interacting as a hydrogen-bonded or “homoconjugated” complex, have been reported (see refs 35–37). No analogous phenomena have been reported for SAMs.

**Table 2. Vibrational Assignments for FTIR-ERS Difference Spectra of Surface-Confined MBA Isomers after Exposure to Vapor-Phase Decylamine<sup>a</sup>**

4-MBA		3-MBA		2-MBA	
energy (cm <sup>-1</sup> )	assignment	energy (cm <sup>-1</sup> )	assignment	energy (cm <sup>-1</sup> )	assignment
3576 w, neg	$\nu_{O-H}$ loss	3576 w, neg	$\nu_{O-H}$ loss	2963 m	$\nu_{a,C-H}(CH_3)$
2967 s	$\nu_{a,C-H}(CH_3)$	2967 s	$\nu_{a,C-H}(CH_3)$	2928 s	$\nu_{a,C-H}(CH_2)$
2925 s	$\nu_{a,C-H}(CH_2)$	2926 s	$\nu_{a,C-H}(CH_2)$	2880 w	$\nu_{s,C-H}(CH_3)$
2879 w	$\nu_{s,C-H}(CH_3)$	2880 w	$\nu_{s,C-H}(CH_3)$	2856 m	$\nu_{s,C-H}(CH_2)$
2854 s	$\nu_{s,C-H}(CH_2)$	2854 m	$\nu_{s,C-H}(CH_2)$	1655–1740 w, br	$\nu_{C=O}$ loss
1740 s, neg; 1710 sh, neg	$\nu_{C=O}$ loss	1743 s, neg; 1708 sh, neg	$\nu_{C=O}$ loss	1618 m	$\nu_{C-C}$ (8b)
1620–1590 w, br	$\delta_{a,N-H}(NH_3^+)$	1632 w, br	$\delta_{a,N-H}(NH_3^+)$	1569 m	$\nu_{C-C}$ (8a)
1591–1582 neg/pos	$\nu_{C-C}$ (8a) shift	1584 m; 1569 neg	$\nu_{C-C}$ (8a loss, 8b gain)	1540 m	$\nu_{a,CO_2^-}$
1540 m	$\nu_{a,CO_2^-}$	1558 m	$\nu_{a,CO_2^-}$	1463 w	$\beta_{a,CH_2}$
1530–1500 w, br	$\delta_{s,N-H}(NH_3^+)$	1530–1500 w, br	$\delta_{s,N-H}(NH_3^+)$	1376 w	$\nu_{s,CO_2^-}$
1469 w	$\beta_{a,CH_2}$	1469 w	$\beta_{a,CH_2}$		
1397 vs; 1355 sh	$\nu_{s,CO_2^-}$	1384 vs; 1403 sh	$\nu_{s,CO_2^-}$		
1360 w, neg	$\beta_{C-H}$ or $\beta_{O-H}$ loss	1185 m neg	$\beta_{C-H}$ or $\nu_{C-O}$ loss		
1168–1189 w, neg	$\beta_{C-H}$ or $\nu_{C-O}$ loss				
1080–1096 m, neg	$\beta_{C-H}$ or $\nu_{C-O}$ loss				
836 m	$\beta_{s,CO_2^-}$				

<sup>a</sup> Key: vs, s, m, w: very strong, strong, medium, weak; sh, shoulder; br, broad; neg, negative; pos, positive. Numbers in parentheses refer to the normal vibrations of the benzene ring for the  $C_{2v}$  point group (in the case of 4-MBA) and the  $C_s$  point group (in the case of 3- and 2-MBA).<sup>40</sup>

charged carboxylate species may be due to concomitant changes in polarization across the benzene ring, the effect of which is dependent on the ring substitution geometry. However, the ring environment is apparently also affected by MBA interactions with the nearby proximity of the metal substrate (*vide supra*), which is likewise geometry dependent.

In the spectral region below 1400 cm<sup>-1</sup> the 4-MBA difference spectra exhibit loss peaks at 1080–1096 cm<sup>-1</sup> and at 1168–1189 cm<sup>-1</sup>, and the 3-MBA difference spectra exhibit a loss peak at 1185 cm<sup>-1</sup>. These loss peaks occur at energies corresponding to substituent-sensitive ring bands ( $\beta_{C-H}$ , Table 1). However, we cannot unequivocally relate these losses to changes in the electron distribution of the ring because monomeric  $\nu_{C-O}$  bands typically occur in the 1080–1180 cm<sup>-1</sup> range. The 2-MBA difference spectra have no loss features whatsoever in this substituent-sensitive region.

In summary, large changes occur in the 4-MBA spectrum upon dosing with decylamine, but these changes are not as prominent in 3-MBA and not resolvable in 2-MBA. This trend is consistent with the data shown in Figures 1 and 2, and it is consistent with increased interactions between acid groups and the surface as the carboxyl group moves closer to the surface.

Some of the loss features in Figure 3 are smaller in magnitude than expected based on examination of *ex-situ* spectra in Figure 1. Most notably, the negative  $\nu_{O-H}$  band in Figure 3a is much smaller than the  $\nu_{O-H}$  peak for unaged 4-MBA (dashed line, Figure 1). Instead, the shape and size of the negative bands in the 4-MBA difference spectra obtained after dosing with decylamine closely resemble the corresponding bands in the spectrum of aged 4-MBA (solid line, Figure 1). The 4-MBA SAM apparently reorders in the flow cell while equilibrating with flowing N<sub>2</sub> prior to dosing, much as this SAM reorders upon aging for 3 h in a H<sub>2</sub>O- and CO<sub>2</sub>-free air environment (Figure 1). This effect is fully reproducible, although the rate and degree of reordering are different for the three different isomers. Because of this apparent structural change, we were careful to obtain *in-situ* FTIR-ERS (Figure 3) and TSMR data under identical experimental conditions.

Parts a–c of Figure 4 show representative plots of frequency shift versus time for TSMRs modified with 4-, 3-, and 2-MBA SAMs, respectively, during exposure to pure N<sub>2</sub> and N<sub>2</sub> containing decylamine vapor. Between 0 and 35 min the device frequency stabilized under a pure

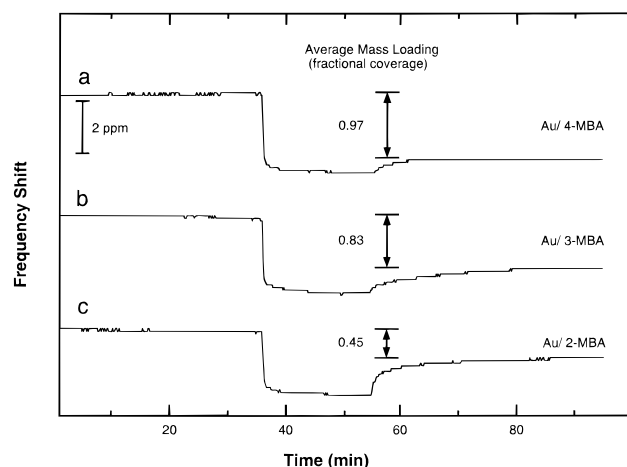


**Figure 4.** Real-time TSMR data obtained from the adsorption of decylamine onto (a) 4-MBA, (b) 3-MBA, and (c) 2-MBA surfaces. The corrected decylamine fractional surface coverages are given in the figure. One part per million corresponds to approximately 9 Hz. See Table 3 for additional information.

**Table 3. Mass/Area Resulting from Dosing MBA SAMs with Decylamine**

	2-MBA	3-MBA	4-MBA
no. of runs	4	5	4
average mass/area (ng/cm <sup>2</sup> ) <sup>a</sup>	66	120	140
average mass loading (fractional coverage) <sup>b</sup>	0.45	0.83	0.97
standard deviation (fractional coverage)	0.05	0.06	0.05

<sup>a</sup> The mass/area calculations do not include the surface roughness factor. <sup>b</sup> The fractional monolayer coverages are referenced to the calculated coverage anticipated to be present on a flat, defect-free Au(111) substrate (0.78 nmol/cm<sup>2</sup>) and incorporate a surface-roughness factor of 1.2.

N<sub>2</sub> purge stream. Between 35 and 55 min the gas stream was switched to 50%-of-saturation decylamine vapor. The negative frequency shift near 35 min corresponds to a mass increase, which the FTIR-ERS data confirm as corresponding to adsorption of decylamine. Between 55 and 95 min the surface was purged with pure N<sub>2</sub> to remove any physisorbed decylamine that might have condensed onto the SAM.

Table 3 summarizes the TSMR results: the average mass/area ratios resulting from decylamine adsorption onto the MBA surfaces are 140, 120, and 66 ng/cm<sup>2</sup> or 0.91, 0.78, and 0.42 nmol/cm<sup>2</sup>, for 4-, 3-, and 2-MBA SAMs,

**Table 4. XPS Measurements of Relative Elemental Surface Coverage for MBA SAMs**

element	PP <sup>a</sup>	peak areas <sup>b</sup>			
		4-MBA	3-MBA	2-MBA	HSC <sub>18</sub>
S <sup>c</sup>	162.4	1.5	1.4	1.5	1.0
O(C=O)	532.5	4.7	3.0	1.5	0
O(C-O)	531.0	2.7	3.8	2.9	0
C(C=O)	288.8	3.5	3.1	2.7 <sup>d</sup>	0
C(C-O)	286.0	4.7	5.4	3.8	0
C	284.6	23.7	21.6	20.2	56.4

<sup>a</sup> Peak position, referenced to C(1s) at 284.6 eV. <sup>b</sup> Peak area corrected for XPS relative atomic sensitivity factor and normalized to the S(2p) intensity of octadecanethiol. <sup>c</sup> Due to depth-dependent photoelectron attenuation,<sup>49,50</sup> sulfur peak intensity is undoubtedly diminished relative to oxygen or carbon peaks. For example, the XPS-measured relative surface coverages for S and C are 1 and 56, respectively, for an HSC<sub>18</sub> (HS(CH<sub>2</sub>)<sub>17</sub>CH<sub>3</sub>) SAM, whereas for an HSC<sub>11</sub> (HS(CH<sub>2</sub>)<sub>10</sub>CH<sub>3</sub>) SAM Bain *et al.* obtained XPS-measured relative surface coverages for S and C of 1 and 32, respectively.<sup>51</sup> <sup>d</sup> Broad peak centered at 288.5 eV.

respectively. The corresponding fractional surface coverages of decylamine are 1.16, 1.00, and 0.54 for 4-, 3-, and 2-MBA, respectively, or, taking into account the surface roughness, the corrected fractional coverages are 0.97, 0.83, and 0.45, respectively. These results are in good agreement with the qualitative FTIR-ERS data: SAMs with the most highly exposed and least hydrogen-bonded acid groups are most receptive to proton transfer. The gravimetric data indicate irreversible binding of decylamine to all three of the SAMs on the time scale of the experiment, in accord with the FTIR-ERS results.

XPS data in the S(2p) region reveal nearly identical surface coverages of the three MBA isomers prior to dosing with decylamine (Table 4). We observe two different states for oxygen in MBA monolayers, which have O(1s) binding

(49) Briggs, D.; Seah, M. P. *Practical Surface Analysis*; Wiley: Chichester, 1983.

(50) Fadely, C. S.; Baird, R. J.; Siekhaus, W. J.; Novakov, T.; Bergstrom, S. A. L. *Electron Spectrosc. Relat. Phenom.* **1974**, *4*, 93.

(51) Bain, C. D.; Troughton, E. B.; Tao, Y. T.; Evall, J.; Whitesides, G. M.; Nuzzo, R. G. *J. Am. Chem. Soc.* **1989**, *111*, 321.

energies of 532.5 (C=O) and 531.0 (C-O) eV. The intensities of the peaks corresponding to O<sub>531.0</sub> relative to O<sub>532.5</sub> are 0.6, 1.3, and 1.9 for the 4-, 3-, and 2-MBA isomers, respectively. We ascribe this increase in the relative intensity of the C-O oxygen peak to an increase in the extent to which the carboxyl-group oxygens interact with the metal surface. XPS results also show that, for 4- and 3-MBA isomers, carbon in the carboxyl group has a binding energy of 288.8 eV. In contrast, the carboxyl group of 2-MBA displays a broad binding-energy peak centered at 288.5 eV. Although the energy shifts in the carboxyl-group carbon are smaller and hence more difficult to detect and interpret than those for oxygen, both results are consistent with our model for 2-MBA monolayers wherein carboxyl-group interaction with the Au surface inhibits proton-transfer reactions with vapor-phase decylamine.

## Conclusions

For monolayers of three different MBA isomers, proximity of the carboxyl group to the Au surface greatly reduces the number and intensities of FTIR-ERS spectral bands and produces changes in the carboxyl-group electronic state. This reflects the effect of interactions between the carboxyl group and the metal surface upon the electron distribution within the surface-confined species. Furthermore, our FTIR-ERS and TSMR results show that proximity of the carboxyl group to the surface reduces MBA reactivity toward a vapor-phase decylamine probe. These results underscore the effect of structure in determining reactivity of, and molecular recognition by, surface-confined monolayers.

**Acknowledgment.** We gratefully acknowledge major support of this work from the National Science Foundation (CHE-9313441). A.J.R. acknowledges support from the U.S. DOE under Contract DE-AC04-94AL85000. M.W. thanks the Patricia Roberts Harris Fellowship Program for graduate fellowship support. We also acknowledge enlightening conversations with Professor Arthur T. Hubbard (University of Cincinnati).

LA9507951